Turbulent heating in an inhomogeneous, magnetized plasma slab

M. Barnes, P. Abiuso

May 14, 2017

Abstract

Observational evidence in space and astrophysical plasmas suggests that more massive charged particles are preferentially heated. One possible mechanism for this is the turbulent cascade of energy from injection to dissipation scales, where the energy is converted to heat. Here we consider a simple system consisting of a magnetized plasma slab of electrons and a single ion species with a cross-field density gradient. We show that such a system is subject to electron drift wave instabilities that are stabilized only when the electron and ion thermal speeds are equal. For unequal thermal speeds, we find that the instability gives rise to turbulent energy exchange between ions and electrons that acts to equalize the thermal speeds. Consequently, turbulent heating tends to equalize the component temperatures of pair plasmas and to heat ions to much higher temperatures than electrons for conventional mass-ratio plasmas.

1 Experimental observations

On a fundamental level, we are interested in determining whether heating due to turbulence drives the plasma toward or away from an equal temperature equilibrium. This is important for plasmas in which the collisional mean free path is much longer than the system size so that thermalization due to collisions is negligible over time scales of interest. Such plasmas include the solar wind and certain accretion flows such as the one at the center of our galaxy. In the case of the solar wind, direct measurements indicate that ions are hotter than electrons and that heavy ions are hotter than light ions. Various possible local heating mechanisms have been proposed, including cyclotron heating, stochastic heating, and reconnection. Furthermore, there are complications due to observed temperature anisotropy which can drive kinetic instabilities such as mirror and firehose. In the case of accretion flows, there is indirect evidence that ions may be much hotter than electrons. If Bondi accretion rate and all gravitational potential energy is converted to thermal energy during accretion, then the estimated temperature is well below that inferred from the observed electron radiation. In this case, either the thermal energy has gone predominantly into the ions or the accretion rate must be much lower than expected.

In what follows we will consider a simple model system in which we can cleanly study the mass and temperature ratio dependence of turbulent heating. Please note that this is currently a work-in-progress. If you are primarily interested in the punchline, see Figs. (3) and (4) and associated discussion.

2 Model system

We consider a system with a straight, homogeneous magnetic field $\mathbf{B} = B\hat{\mathbf{z}}$ and a density gradient perpendicular to the field in the x-direction. We restrict our attention to electrostatic fluctuations whose frequency is small compared with the Larmor frequency and adopt the gyrokinetic ordering:

$$\frac{\omega}{\Omega_s} \sim \frac{k_\parallel}{k_\perp} \sim \frac{\rho_s}{L_n} \sim \frac{\delta f_s}{f_s} \sim \frac{q_s \varphi}{T_s} \sim \epsilon, \tag{1}$$

where φ is the electrostatic potential fluctuation, f_s is the distribution function for species s, δf is the fluctuating component of f, ω is the characteristic frequency of the turbulent fluctuations, $k_\parallel$ and $k_\perp$ are the associated wavenumbers along and across the mean field, Ω_s is the Larmor frequency for species s, ρ_s its thermal Larmor radius, T_s its temperature, q_s its charge, and L_n is the mean density gradient scale length.

Applying these orderings to the Vlasov equation and averaging over the rapid gyration of particles about the mean magnetic field results in the gyrokinetic equation,

$$\frac{\partial h_s}{\partial t} + v_\parallel \frac{\partial h_s}{\partial z} + \frac{c}{B}\{\langle \varphi \rangle_{\mathbf{R}_s}, h_s\} = \frac{q_s}{T_s}\frac{\partial \langle \varphi \rangle_{\mathbf{R}_s}}{\partial t} F_{M,s} + \frac{c}{B}\frac{\partial \langle \varphi \rangle_{\mathbf{R}_s}}{\partial y}\frac{\partial \ln n_{0,s}}{\partial x} F_{M,s}, \tag{2}$$

where $h_s = \delta f_s + (q_s \varphi / T_s) F_{M,s}$ is the non-Boltzmann piece of δf_s, t is time, $v_\parallel$ is the parallel component of the particle velocity, c is the speed of light, $F_{M,s}$ is the Maxwellian velocity distribution associated with the mean component of f, n_0 is the mean density, $\{\}$ indicates a Poisson bracket, and $\langle \varphi \rangle_{\mathbf{R}_s}$ is the average of φ over Larmor angle at fixed guiding center position $\mathbf{R}$.

The gyrokinetic system is closed by imposing quasineutrality:

$$\sum_s q_s \int d^3 v \delta f_s = 0. \tag{3}$$

2.1 Turbulent heating

At next order in the small parameter ϵ, one obtains an equation for the slow evolution of the mean temperature T_0:

$$\frac{3}{2} n_0 \frac{dT_{0,s}}{dt} = H_s + C_s, \tag{4}$$

where C_s represents collisional temperature equilibration, and the turbulent heating H_s is given by

$$H_s = \frac{1}{V} \int d^3R \int_{\mathbf{R}} d^3v q_s h_s \frac{\partial \langle \varphi \rangle_{\mathbf{R}_s}}{\partial t}. \tag{5}$$

Here V is the volume over which the spatial average is performed and the subscript $\mathbf{R}$ on the velocity integration indicates that it is carried out at fixed $\mathbf{R}$. For systems with a sufficiently long collisional mean free path, the collisional temperature equilibration rate can be ignored, and the temperature of each plasma species will be determined solely by the turbulent heating H_s. Expressing Eq. (7) in terms of Fourier modes gives

$$\overline{H_s} = q_s \sum_{\mathbf{k}} \frac{\partial \varphi_{\mathbf{k}}}{\partial t} \int d^3v \hat{h}^*_{\mathbf{k},s} J_0(\alpha_{k_\perp,s}), \tag{6}$$

where $\alpha_{k_\perp,s} \doteq k_\perp v_\perp / \Omega_s$ and J_0 is a Bessel function of the first kind.

When the turbulence is in a steady state, one is interested in the time average of H_s. Averaging Eq. (5) over a timescale long compared to the nonlinear time provides an alternative expression for H_s:

$$\overline{H_s} = \frac{1}{2V} \int d^3R \int_{\mathbf{R}} d^3v q_s \overline{\left(h_s \frac{\partial \langle \varphi \rangle_{\mathbf{R}_s}}{\partial t} - \frac{\partial h_s}{\partial t} \langle \varphi \rangle_{\mathbf{R}_s} \right)}, \tag{7}$$

with the overline denoting a time average. The form for turbulent heating given by Eq. (7) ensures that the net (species-summed) turbulent heating is zero in the absence of an external energy injection mechanism at each instant in time.

3 Linear analysis

If we consider small amplitude perturbations, we may neglect the quadratic nonlinearity and carry out a linear analysis of the gyrokinetic equation. Assuming solutions of the form $h_s = \sum_{\mathbf{k}} \hat{h}_{\mathbf{k},s}(v_\parallel, v_\perp) \exp(i\mathbf{k} \cdot \mathbf{R}_s - i\omega t)$, we obtain

$$\hat{h}_{\mathbf{k},s} = \frac{q_s \hat{\varphi}_{\mathbf{k}}}{T_s} J_0(\alpha_{k_\perp,s}) \left(\frac{\omega + \omega_{*,s}}{\omega - k_\parallel v_\parallel} \right) F_{M,s}, \tag{8}$$

where m_s is species mass, $v_{\mathrm{th},s} = 2T_s/m_s$, $\rho_s = v_{\mathrm{th},s}/|\Omega_s|$, $L_{n,s} = -\partial \ln n_{0,s}/\partial x$, and

$$\omega_{*,s} = \frac{k_y \rho_s v_{\mathrm{th},s}}{2L_{n,s}} \frac{q_s}{|q_s|}. \tag{9}$$

From quasineutrality

$$\int d^3v \, (h_i - h_e) = \frac{e^2 n}{T_e} (1 + \tau) \varphi, \tag{10}$$

where $\tau \doteq T_e/T_i$, and we have restricted our attention to a single ion species with proton charge e. Substituting Eq. (8) into Eq. (10) results in the dispersion relation

$$\epsilon(\omega, \mathbf{k}) = 1+\tau+\left(\zeta_e - \frac{k_y \rho_e}{2k_\parallel L_n}\right)\Gamma_0(k_y\rho_e) Z\left(\zeta_e\right)+\tau\left(\zeta_i + \frac{k_y \rho_i}{2k_\parallel L_n}\right)\Gamma_0\left(k_y\rho_i\right) Z\left(\zeta_i\right) = 0, \tag{11}$$

where $\zeta_s \doteq \omega/k_\parallel v_{\mathrm{th},s}$,

$$Z(x) \doteq \mathrm{i}\sqrt{\pi}\mathrm{e}^{-x^2}\ \mathrm{erfc}\left(-\mathrm{i}x\right) \tag{12}$$

is the plasma dispersion function, erfc is the complementary error function, and

$$\Gamma_0(x) \doteq \exp\left(-\frac{x^2}{2}\right) I_0\left(\frac{x^2}{2}\right), \tag{13}$$

with I_0 a modified Bessel of the first kind. Note that we have used quasineutrality to set $L_{n,i} = L_{n,e} \doteq L_n$.

3.1 Quasilinear energy exchange

Using Eq. (8) for $\hat{h}_{\mathbf{k},s}$ in Eq. (7), we get a quasilinear approximation for the energy exchange:

$$\begin{aligned} H_s = \sum_{\mathbf{k}} H_{\mathbf{k}} &= -\frac{q_s^2}{T_s}\sum_{\mathbf{k}} i\omega\left|\varphi_{\mathbf{k}}\right|^2 \int d^3v \left(\frac{\omega^* + \omega_{*,s}}{\omega^* - k_\parallel v_\parallel}\right) F_{M,s} J_0^2(\alpha_{k_\perp,s}) \\ &= \frac{q_s^2 n_s}{T_s}\sum_{\mathbf{k}} i\omega\left|\varphi_{\mathbf{k}}\right|^2 \Gamma_0(k_\perp\rho_s)\left(\frac{k_y\rho_s}{2k_\parallel L_n}\frac{q_s}{|q_s|} + \zeta_s^*\right) Z(\zeta_s^*). \end{aligned} \tag{14}$$

This expression will be dominated by the mode with the largest linear growth rate and its complex conjugate:

$$H_s \approx 2\mathrm{Re}\left(H_{\mathbf{k}_m}\right) = -2\frac{q_s^2 n_s}{T_s}\left|\varphi_{\mathbf{k}_m}\right|^2 \Gamma_0(k_{\perp,m}\rho_s)\mathrm{Im}\left(\omega_m\left(\frac{k_y\rho_s}{2k_\parallel L_n}\frac{q_s}{|q_s|} + \zeta_{s,m}^*\right) Z(\zeta_{s,m}^*)\right), \tag{15}$$

where $\mathbf{k}_m$ indicates the wavevector at which the maximum growth rate occurs and $\omega_m = \omega(\mathbf{k}_m)$. From Eq. (15), we see that the quasilinear estimate for the turbulent energy exchange depends on the frequency of the fastest growing mode. In the following subsections we obtain numerical and approximate analytical solutions for these frequencies in various limits.

3.2 Comparable thermal speeds

We first show that there is no instability, and thus no turbulent heating, if $v_{\mathrm{th},e} = v_{\mathrm{th},i}$. To find the condition for marginal stability, we seek solutions for which $\gamma \doteq \mathrm{Im}\left(\omega\right) = 0$. In this case, the plasma dispersion function simplifies to

$Z(\zeta) = \sqrt{\pi}\exp(-\zeta^2)(\mathrm{i} - \mathrm{erfi}\,(\zeta))$, with erfi the imaginary error function. The constraint $\mathrm{Im}\,(\epsilon) = 0$ then gives

$$\left(\zeta_e - \frac{k_y\rho_e}{2k_\parallel L_n}\right)\Gamma_0(k_y\rho_e)\exp(-\zeta_e^2) = -\tau\left(\zeta_i + \frac{k_y\rho_i}{2k_\parallel L_n}\right)\Gamma_0\left(k_y\rho_i\right)\exp(-\zeta_i^2). \tag{16}$$

Substituting this expression into the constraint $\mathrm{Re}\,(\epsilon) = 0$ gives

$$0 = 1 + \tau + \tau\left(\zeta_i + \frac{k_y\rho_i}{2k_\parallel L_n}\right)\Gamma_0\left(k_y\rho_i\right)\pi^{1/2}\exp(-\zeta_i^2)\left(\mathrm{erfi}\,(\zeta_e) - \mathrm{erfi}\,(\zeta_i)\right). \tag{17}$$

When $v_{\mathrm{th},e} = v_{\mathrm{th},i}$, as would be the case for an equal temperature pair plasma or for a more conventional mass ratio plasma with ions much hotter than electrons, then $\zeta_e = \zeta_i$, and Eq. (17) has no solution. Such a plasma is therefore universally stable.

Next, we consider how marginal stability is modified when $v_{\mathrm{th},e} = v_{\mathrm{th},i}\,(1+\delta)$, with $|\delta| \ll 1$. In this limit, the constraint Eq. (17) becomes

$$0 \approx 1 + \tau - 2\tau\zeta_i\Gamma_0(k_y\rho_i)\left(\zeta_i + \frac{k_y\rho_i}{2k_\parallel L_n}\right)\delta, \tag{18}$$

with solutions given by

$$\zeta_i = -\frac{k_y\rho_i}{4k_\parallel L_n} \pm \frac{\sqrt{\left(\tau k_y\rho_i\Gamma_0(k_y\rho_i)\delta\right)^2 + 8\delta(1+\tau)\tau\Gamma_0(k_y\rho_i)(k_\parallel L_n)^2}}{4\tau k_\parallel L_n\Gamma_0(k_y\rho_i)\delta}. \tag{19}$$

In order for the solutions to be real (as we assumed when we considered marginal stability), the term inside the square root must be positive definite. This constraint is satisfied when $\delta > 0$ or when $\tau(k_y\rho_i)^2\Gamma_0(k_y\rho_i)|\delta| > 8(1+\tau)(k_\parallel L_n)^2$. The latter constraint can always be satisfied for large enough values of $k_y/k_\parallel$. Consequently, we see that there can be instability for all values of δ; i.e., for all plasmas with $v_{\mathrm{th},i} \neq v_{\mathrm{th},e}$.

We now consider the two cases of pair plasmas ($m_e = m_i$) and conventional mass ratio plasmas ($m_e \ll m_i$) separately to determine how the plasma instability affects the turbulent heating and thus the electron-ion temperature ratio.

3.3 Conventional mass ratio

For plasmas with $m_i \gg m_e$, there will be disparate thermal speeds $v_{\mathrm{th},i} \ll v_{\mathrm{th},e}$ for temperature ratios satisfying $m_e/m_i \ll \tau \ll m_i/m_e$. In this case, we can look for solutions to the dispersion relation that satisfy $|\zeta_e| \ll 1 \ll |\zeta_i|$. With this restriction, the plasma dispersion functions appearing in Eq. (11) can be greatly simplified. In particular, we use

$$Z\left(\zeta_e\right) \approx \mathrm{i}\sqrt{\pi} \tag{20}$$

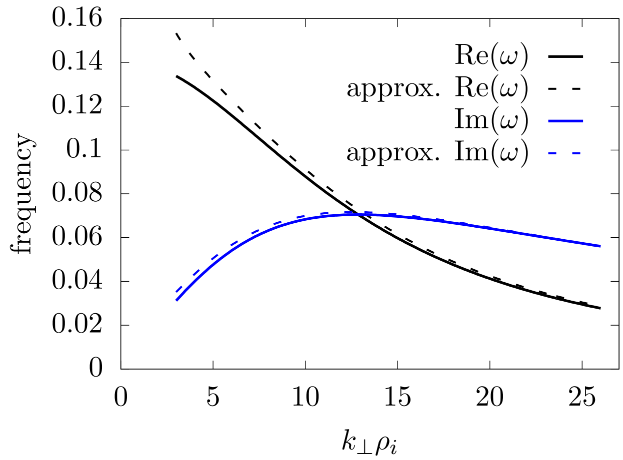

Figure 1: Comparison of exact (solid lines) and approximate analytical (dashed lines) growth rates for the case $\tau = 1$ and $m_i/m_e = 337824$ (tungsten ions).

and

$$Z(\zeta_i) \approx -1/\zeta_i, \tag{21}$$

giving the following approximate dispersion relation:

$$\zeta_i\left(1+\tau\right) + \zeta_i\left(\zeta_e - \frac{k_y\rho_e}{2k_\parallel L_n}\right)\Gamma_0(k_y\rho_e)\mathrm{i}\sqrt{\pi} - \tau\left(\zeta_i + \frac{k_y\rho_i}{2k_\parallel L_n}\right)\Gamma_0\left(k_y\rho_i\right) = 0. \tag{22}$$

We next consider wavelengths much shorter than the ion Larmor radius but much longer than the electron Larmor radius; i.e., $k_\perp\rho_i \gg 1 \gg k_\perp\rho_e$. In this limit we can approximate $\Gamma(k_y\rho_e) \approx 1$ and $\Gamma(k_y\rho_i) \approx 1/(\sqrt{\pi}k_\perp\rho_i)$ in Eq (22) to obtain

$$\zeta_i\left(1+\tau\right) + \zeta_i\left(\zeta_e - \frac{k_y\rho_e}{2k_\parallel L_n}\right)\mathrm{i}\sqrt{\pi} - \frac{\tau}{\sqrt{\pi}}\left(\frac{\zeta_i}{k_\perp\rho_i} + \frac{k_y}{k_\perp}\frac{1}{2k_\parallel L_n}\right) = 0. \tag{23}$$

Seeking solutions for which $\zeta_i \sim k_\perp\rho_e/k_\parallel L_n$ allows us to neglect the ζ_e and $\zeta_i/k_\perp\rho_i$ terms. The resultant solution for ω is

$$\omega = \frac{\tau k_\parallel v_{\mathrm{th},i}}{\sqrt{\pi}}\frac{2k_\parallel L_n\left(1+\tau\right)\mathrm{sgn}(k_y) + \mathrm{i}\sqrt{\pi}k_\perp\rho_e}{\left(1+\tau\right)^2\left(2k_\parallel L_n\right)^2 + \pi k_\perp^2\rho_e^2}. \tag{24}$$

In Fig. (1) we show an example comparison of the exact and analytical expressions for ω. In Fig. (2) we give the growth rates as a function of mass ratio for $\tau = 1$ and as a function of τ for an electron-proton plasma.

Eq. (24) indicates that for $k_\parallel > 0$ there is an instability with peak growth rate γ at wavelengths satisfying $\partial\gamma/\partial k_\parallel = \partial\gamma/\partial k_\perp = 0$. These constraints give

$$k_{\perp,m}\rho_e = \frac{2}{\sqrt{\pi}}k_\parallel|L_n|\left(1+\tau\right), \tag{25}$$

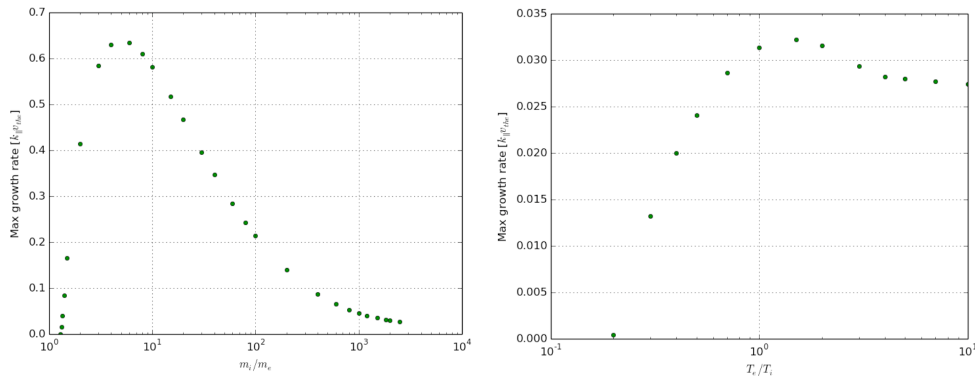

Figure 2: Linear growth rates normalized by $k_\parallel v_{\mathrm{th},e}$ from `GS2` as a function of (left) ion-electron mass ratio with $T_e = T_i$ and (right) electron-ion temperature ratio with a proton-electron plasma.

so that

$$\omega_m = \frac{\tau}{4\sqrt{\pi}\,(1+\tau)} \frac{v_{\mathrm{th},i}}{|L_n|} \left(\mathrm{i} + \mathrm{sgn}(k_y L_n)\right), \tag{26}$$

with ω_m the complex frequency evaluate at $\mathbf{k}_m$.

Plugging Eq. (26) for ω_m into Eq. (15) for turbulent heating and using the appropriate approximations for $\Gamma(k_y \rho_s)$ and $Z(\zeta_s)$ gives

$$\begin{aligned} H_i = -H_e &\approx -\frac{2e^2 n}{T_e} \left|\varphi_{\mathbf{k}_m}\right|^2 \mathrm{Re}\left(\omega_m\right) \frac{\omega_{*,e}}{k_\parallel v_{\mathrm{th},e}} \sqrt{\pi} \\ &= \frac{e^2 n}{T_i} \left|\varphi_{\mathbf{k}_m}\right|^2 \frac{1}{2\sqrt{\pi}} \frac{v_{\mathrm{th},i}}{|L_n|} > 0. \end{aligned} \tag{27}$$

So ions are heated and electrons are cooled; i.e., the instability acts to equalize $v_{\mathrm{th},e}$ and $v_{\mathrm{th},i}$ and thus stabilize the mode. This is shown in Fig. (3), where the quasilinear heating calculated from linear GS2 simulations is given as a function of m_i/m_e for $\tau = 1$ and as a function of τ for an electron-proton plasma. We see that the ion heating is positive-definite for both cases, in agreement with our approximate analytic result.

3.4 Pair plasmas

We have shown analytically that there can only be instability – and thus turbulent heating – for pair plasmas when the component temperatures are unequal. This is confirmed by linear simulations from GS2 for an electron-positron plasma, as shown in Fig. (4). The quasilinear estimate for turbulent heating taken from linear GS2 simulations is also shown in Fig. (4), as well as some preliminary results for turbulent heating taken from nonlinear simulations. In both cases, the turbulent heating is such that it drives the thermal speeds of the electron and positrons together; i.e., it acts to shut off the instability.

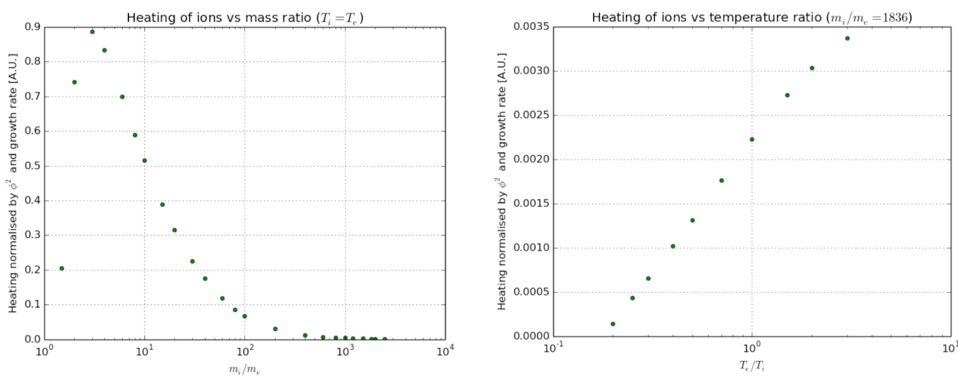

Figure 3: Ratio of ion turbulent heating H_i to $|\varphi|^2$ from linear GS2 simulations weighted by the corresponding max linear growth rates. (Left): electron-ion mass ratio scan with $T_i = T_e$; (Right): temperature ratio scan for an electron-proton plasma.

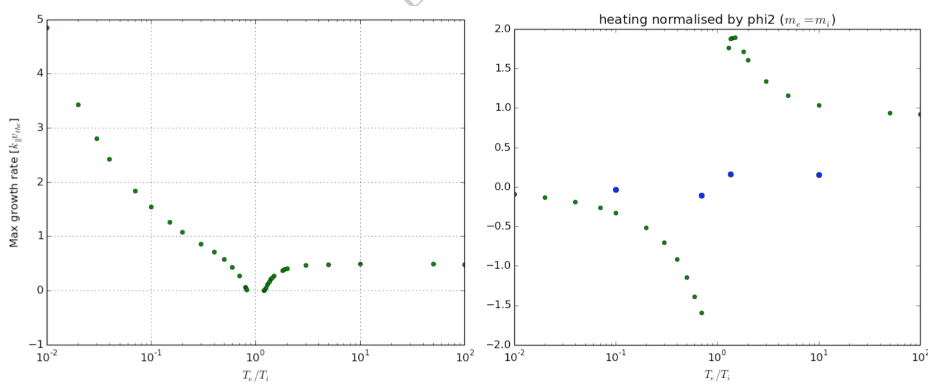

Figure 4: (Left): Linear growth rates normalized by $k_\| v_{\mathrm{th},e}$ from `GS2` as a function of electron-ion temperature ratio with an electron-positron plasma. (Right): τ dependence of turbulent heating for an electron-positron plasma from a quasilinear estimate (green) with turbulent heating normalized by $|\varphi|^2$ for the max linear growth rate and from preliminary nonlinear simulations (blue).

4 Conclusions

The analytical and numerical results shown in this paper indicate that turbulent heating driven by the electron drift wave instability present in an inhomogeneous, magnetized plasma acts to stabilize the mode. Stabilization occurs when the ion and electron thermal speeds are equal. For a conventional mass ratio plasma with $T_i \sim T_e$, this leads to the ions being heated and the electrons cooled; for a pair plasma, the turbulent heating acts to equalize the ion and electron temperatures.

These conclusions are largely based on linear theory and simulations. Work is currently under way to verify these results with nonlinear simulations.